

First Images of Asteroid 243 Ida

M. J. S. Belton, C. R. Chapman,* J. Veverka, K. P. Klaasen, A. Harch, R. Greeley, R. Greenberg, J. W. Head III, A. McEwen, D. Morrison, P. C. Thomas, M. E. Davies, M. H. Carr, G. Neukum, F. P. Fanale, D. R. Davis, C. Anger, P. J. Gierasch, A. P. Ingersoll, C. B. Pilcher

The first images of the asteroid 243 Ida from Galileo show an irregular object measuring 56 kilometers by 24 kilometers by 21 kilometers. Its surface is rich in geologic features, including systems of grooves, blocks, chutes, albedo features, crater chains, and a full range of crater morphologies. The largest blocks may be distributed nonuniformly across the surface; lineaments and dark-floored craters also have preferential locations. Ida is interpreted to have a substantial regolith. The high crater density and size-frequency distribution (-3 differential power-law index) indicate a surface in equilibrium with saturated cratering. A minimum model crater age for Ida—and therefore for the Koronis family to which Ida belongs—is estimated at 1 billion years, older than expected.

The five images of 243 Ida (1), returned after Galileo's 28 August 1993 encounter with the asteroid (2), allow a preliminary characterization of its global properties and its surface geology. In comparison with 951 Gaspra, the first asteroid encountered by Galileo (3, 4), Ida is more than twice as large, spins twice as fast, has a much higher pyroxene/olivine ratio, and is a member of the Koronis family, a well-defined, populous group of asteroids with similar orbital properties. The spacecraft's Solid-State Imaging (SSI) system (5) acquired a total of 150 images comprising 18 different views of the asteroid (many through multiple filters). The first five frames that show Ida are part of a high-resolution mosaic (Fig. 1) taken with no filter ("clear" filter) between 4 and 2.5 min before encounter, while the spacecraft was between about 3800 and 3100 km

from Ida. The solar phase angle varies in these frames from 48° to 60° , and the surface resolution varies from 38 to 31 m per pixel. In one area, there is substantial overlap between two of the images, which provides an 8-km swath of stereoscopic coverage at a convergence angle of about 10° . The purpose of this article is to present our preliminary analysis of this mosaic; although many of the features we discuss may be seen in our illustrations, others were studied with image processing techniques and may not be readily apparent in these pictures.

Rotation and General Appearance

As expected from telescopic observations, Ida shows an irregular, elongated shape. A 56 km by 24 km by 21 km ellipsoid roughly

fits the visible limb and terminator, $\sim 5\%$ larger than ground-based estimates. This model shows root-mean-square (rms) deviations with respect to the visible limb of ± 2 km or 14% of the mean radius. There are no obvious indications of a large-scale binary or compound structure, and it appears, as seen from this side, as though it could be a coherent, single body; on the other hand, it is highly angular, obviously modified by impact processes, and shows lineaments that could indicate fractures. The appropriate rotation pole (6) can be immediately selected from the two ambiguous poles determined from ground-based data by Ida's shape and orientation (Fig. 2). Although these images cover only 1.9° of rotation, displacement of shadows in overlap regions already confirms retrograde rotation. The landscape of the eastern region (see Fig. 3 for orientation) is dominated by five large (~ 5 to 8 km) bowl-shaped craters; the central region is reminiscent of the large planar facets seen on Gaspra (3, 4). The ruggedness of the terrain is indicated by the frequent occurrence of strongly foreshortened craters away from the limb and in the region of stereoscopic overlap between frames D and E (Fig. 3), which covers a ridge separating two large craters. Because only $\sim 30\%$ of Ida's surface is visible in this

M. J. S. Belton is at National Optical Astronomy Observatories, Tucson, AZ 85719, USA. C. R. Chapman and D. R. Davis are with the Planetary Science Institute—Science Applications International Corporation (SAIC), Tucson, AZ 85705, USA. J. Veverka, P. C. Thomas, and P. J. Gierasch are in the Department of Astronomy, Cornell University, Ithaca, NY 14853, USA. K. P. Klaasen and A. Harch are at the Jet Propulsion Laboratory, California Institute of Technology, Pasadena, CA 91109, USA. R. Greeley is in the Department of Geology, Arizona State University, Tempe, AZ 85287-1404, USA. R. Greenberg is at the Lunar and Planetary Laboratory, University of Arizona, Tucson, AZ 87721, USA. J. W. Head III is in the Department of Geology, Brown University, Providence, RI 02912, USA. A. McEwen is with the United States Geological Survey, Flagstaff, AZ 86001, USA. D. Morrison is at the National Aeronautics and Space Administration Ames Research Center, Moffett Field, CA 94035, USA. M. E. Davies is with RAND, Santa Monica, CA 90406, USA. M. H. Carr is with the United States Geological Survey, Menlo Park, CA 94025, USA. G. Neukum is with the Deutsche Forschungsanstalt für Luft und Raumfahrt, Institute for Planetary Exploration, Berlin, Germany. F. P. Fanale is with the Institute of Geophysics, University of Hawaii, Honolulu, HI 96822, USA. C. Anger is with the Institute for Space and Terrestrial Science, Concord, Ontario, Canada L4K 3C8. A. P. Ingersoll is at the California Institute of Technology, Pasadena, CA 91125, USA. C. B. Pilcher is with the National Aeronautics and Space Administration, Washington, DC 20546, USA.

*To whom correspondence should be addressed.

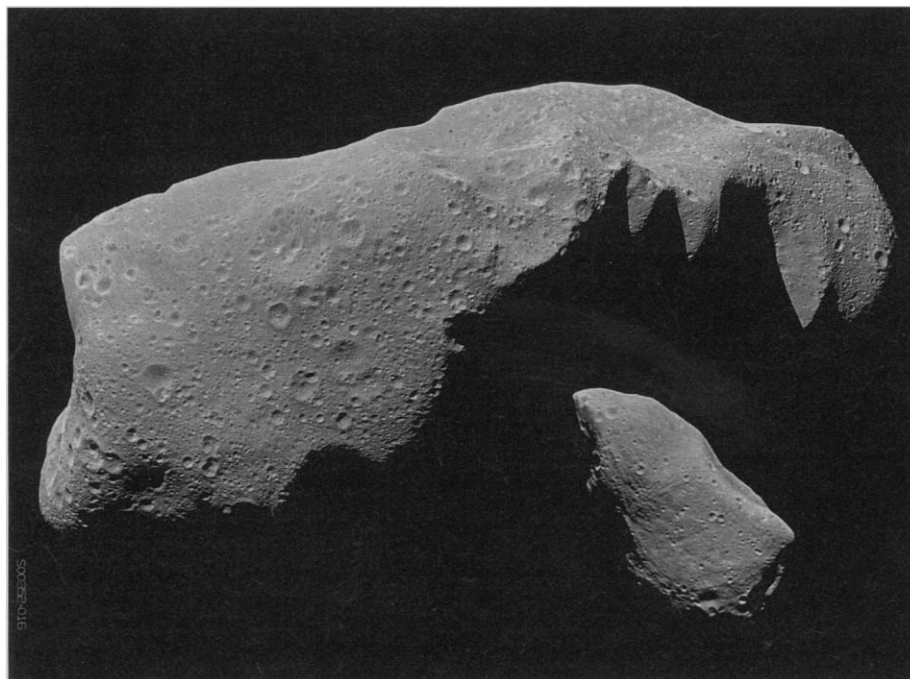


Fig. 1. Mosaic of Ida with Gaspra included (lower right), at the same scale, for comparison.

mosaic, a more detailed description of Ida's large-scale properties must await more complete rotational coverage in images that have recently been returned from the spacecraft, but not yet analyzed.

Craters

Crater morphology. The ubiquitous presence of impact craters clearly indicates that collisions are the principal geologic process shaping the surface of Ida. Most craters have a simple bowl shape, with a only few showing flat, sometimes crenulated floors. Several may have central mounds; these are associated with the rims of large craters and may be simply a chance effect of a substratum of blocky rim material. There is a continuous range of degradation states (Fig. 4). A few of the craters that appear freshest (that is, have the sharpest, least degraded shapes) have one or two short rays extending to ~ 1 crater diameter; however, most craters with crisp rims do not have rays, and there is an absence of distinct, localized ejecta blankets, as expected for an object with low surface gravity (7). A few craters have polygonal shapes, and others have straight rim segments, suggesting formation in a fractured layer or one with significant preexisting stresses. In an area of high sun illumination (western region) is a cluster of apparently dark-floored craters, some surrounded by a halo of brighter material. Stratification in the near-surface materials

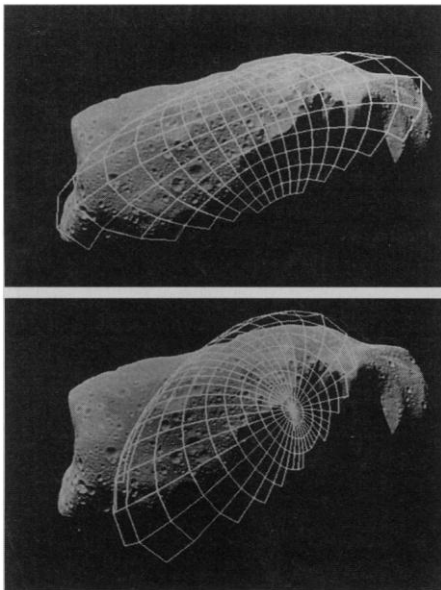


Fig. 2. Ida with a model ellipsoid superposed and oriented according to the two possible rotation poles (6). The solution in the top panel, with the north pole in the direction of a right ascension of 50.25° and a declination of 76.32° (J2000), is clearly preferred. The retrograde rotation is in the sense that the right-hand (eastern) part of Ida is swinging out of the paper, toward the viewer, while the left-hand part is receding.

and the presence of a regolith are possible interpretations.

Crater chains. There are several linear chains of three or more craters of similar size. They range from 500 m to 2.5 km in length, with component craters in the 200- to 400-m size range; their orientations and locations seem random, suggesting impacts by clusters of projectiles, perhaps trains of ejecta from other cratering impacts.

Size-frequency distribution. The differential size-frequency relation for the crater

population on Ida (8) is shown in Fig. 5A. Cumulative frequencies are plotted in Fig. 5B for three different morphological classes of craters (fresh, intermediate, and degraded, as estimated visually along the continuum from apparently pristine to highly modified). The overall slope (exponent of a differential power-law fit to the data) is -3.3 in the range of diameters from 200 m to 3 km, considerably shallower than that for Gaspra (3, 4); for craters < 1 km in diameter, it is near the -3.0 slope charac-

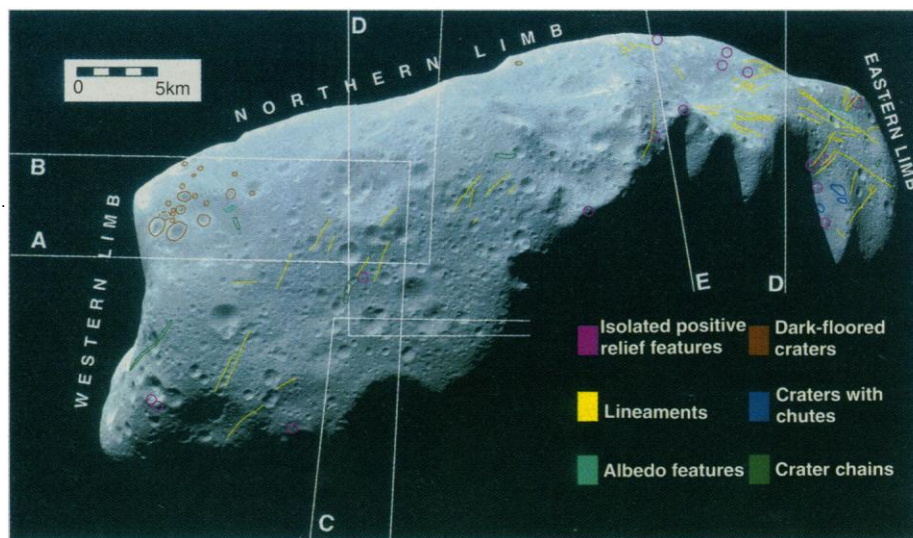


Fig. 3. Map of geological features on Ida. Locations of the five frames that make up the Ida picture [command times in UTC (hours:minutes:seconds), phase in degrees, and range in kilometers]: (A) 16:47:56.266, 48.3, 3821; (B) 16:48:04.933, 49.3, 3738; (C) 16:48:13.600, 50.3, 3656; (D) 16:48:22.266, 51.3, 3575; and (E) 16:49:22.933, 60.0, 3057. The major regions used in the text are identified.

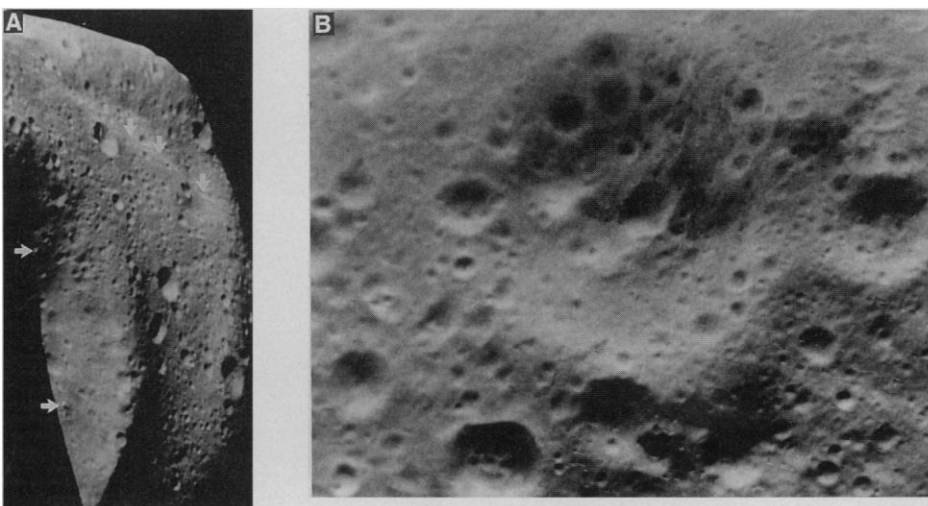


Fig. 4. Examples of a groove, boulders, and a range of crater degradation states. (A) Enlargement of the eastern end of Ida showing the location of several prominent boulders (arrows at left), on the inner wall of a large crater, and a prominent groove (arrows at top), extending for at least 3 km. The image is ~ 12 km in height; north is approximately toward the top. (B) Range of crater degradation states in the western central region of Ida. The large central crater is ~ 4.5 km in diameter and has been modified by many subsequent impacts on its rim and in its interior, as has the smaller crater on its eastern rim. Several relatively fresh craters with linear rim crests are along or beyond its southern rim. The image is ~ 8.5 km wide; north is toward the top.

teristic of equilibrium by crater-upon-crater "saturation" by projectile populations having slopes steeper than -3.0 (9). The approximately parallel relations found for the three morphological classes are expected for saturation equilibrium (10). Although statistics are poor, an R plot comparing Ida crater densities with other bodies (Fig. 5C) indicates that frequencies of craters >1 km in diameter may begin to depart below saturation equilibrium densities. In that case, the population of larger craters, yet to be revealed in the remaining images of Ida, may directly reflect the population of projectiles rather than the equilibrium size distribution that results from the preferential loss of smaller craters from overlap and erosion by the saturation of still smaller craters.

Cratering "age." At diameters of ≥ 1 km, the crater density is about five times greater on Ida than on Gaspra, whose surface age has been estimated at ~ 200 million years (3, 4). It is expected that Gaspra and Ida, although they are in somewhat different parts of the asteroid belt, are subject to impact by roughly the same population of projectiles. Studies of the orbital distributions of larger asteroids (11) show that over half of the objects that could intersect one body would intersect the other, and vice versa, with similar impact velocities. Because the smaller projectiles responsible for cratering are believed to be the widely dispersed collisional fragments of larger asteroids, the cratering flux hitting both bodies should be roughly the same (this extrapolation is an assumption that bears critical evaluation). Assuming that the impact rate on both bodies has been the same and

constant with time, there are two possible interpretations for the different crater populations: (i) The strength of the surface material is much greater on Gaspra and projectiles make smaller craters on Gaspra than on Ida; or (ii) projectiles make the same size craters on both bodies, but Ida's surface is about five times older than Gaspra's. While emphasizing that the first interpretation cannot, at present, be ruled out, we prefer the second, which yields a rough estimate of the minimum age for exposure of Ida's surface to asteroidal projectiles of ~ 1 billion years. Because Ida is a member of the Koronis family, it must have been created as a fragment from the catastrophic disruption of the precursor body no earlier than that, so 1 billion years would seem to be a minimum age for the Koronis family as a whole. This is older than the expectations of Binzel (12) and others, which are based on considerations of the dynamics of the Koronis family.

Blocks, Chutes, Grooves, and Regolith

Blocks. Many isolated positive relief features are evident on the surface. Among them, we have confidently distinguished about 20 blocky features larger than 1 pixel across, which distinctly contrasts with their local background (most are indicated in Fig. 3). Six of the blocks are larger than 100 m across; the largest are ~ 150 m (~ 4 pixels) long, similar to the maximum sizes of blocks found on Phobos, Deimos, and the moon (13). Generally it is not possible to say whether they are perched on the surface or

partially buried larger objects. However, at least one object has an associated trail suggestive of a low-velocity impact by a block now sitting on the surface or of a dislodged boulder rolling across the surface. The spatial distribution of clearly identified blocks is nonuniform. There is a clustering of the majority in the eastern region, many within the two largest (~ 8 km in diameter) craters that define Ida's shape in that region. There is a possible second cluster of blocks near the western end of Ida. In contrast, no blocks were identified with such high confidence in the well-imaged central region nor along Ida's limb, outside of the large craters. The spatial nonuniformity seems to be real, despite potential biases associated with the variable lighting geometry and resolution across the mosaic, foreshortening, smear, and local topographic effects.

Blocks are likely to be impact ejecta and to be the largest components of a size distribution of particles that make up Ida's regolith. Their emplacement on the surface may have been affected by the rapid rotation of Ida, which substantially reduces the effective gravity at the two ends of the asteroid (7). Preliminary calculations indicate that blocks launched randomly from the surface at velocities just below the escape velocity, which achieve temporary orbit around Ida, will impact preferentially on the leading rotational face (which coincides roughly with the eastern region), just as observed. Some blocks may have followed suborbital trajectories to their present positions. Alternatively, block distribution could reflect underlying lithology or regolith thickness. Some of the numerous blocks

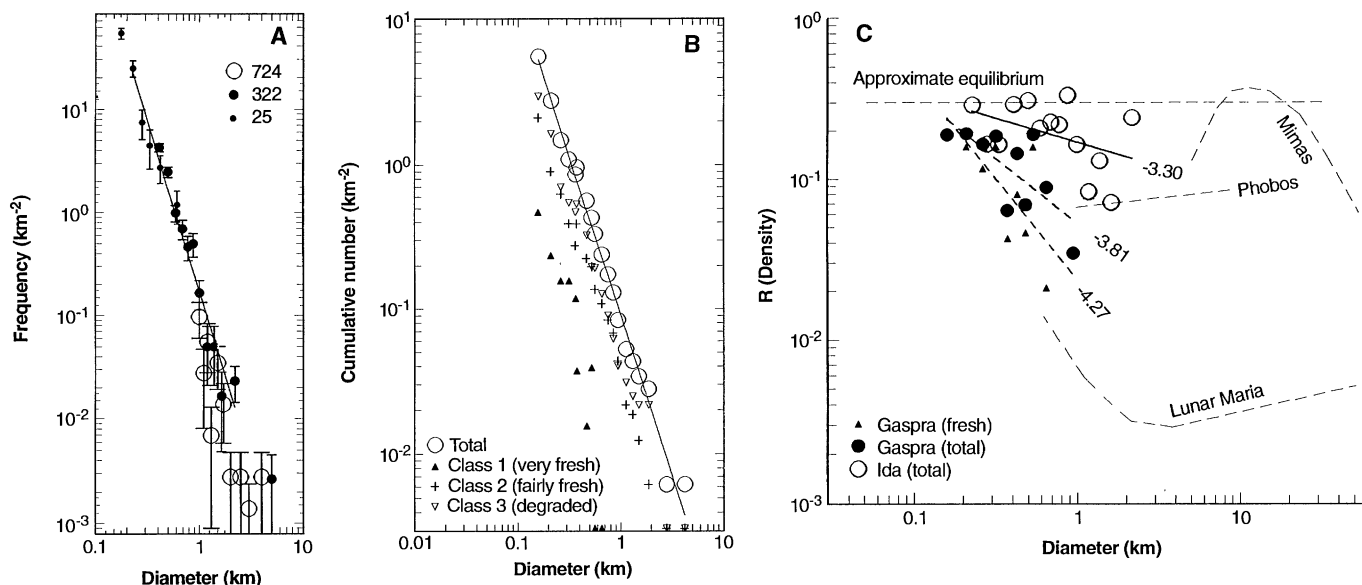


Fig. 5. (A) Differential size-frequency relations were sampled in three different counting regions (25, 322, and 724 km^2). Incomplete data at small diameters have been omitted. The line is a least squares fit to the solid data points and has a slope of -3.3 . (B) Cumulative size-frequency relations for all craters and for the three morphological classes noted in the text. (C) R plot of crater

densities (differential crater frequencies from the two smaller counting areas divided by the cube of the diameter). Ida data are shown as open circles. The horizontal line has been set at a density of 0.3, which is typical of the most heavily cratered terrains known on planetary satellites.

located near or within large impact craters may be directly associated with them (for example, excavated by them or exposed by mass wasting).

Because of their relatively small size, blocks have only a short lifetime against collisional disruption, about 30 million to 80 million years for the largest ones (14). Their presence on the surface indicates that one or more craters in the 1- to 10-km size range were formed during the last 30 million to 80 million years (only impacts that produce craters in this size range can be expected to produce 100-m-sized blocks).

Linear features. Lineaments are relatively common on Ida, including systems of grooves, albedo stripes, and short crater chains. The most prominent system of grooves (linear depressions of uniform width) is located at the eastern limb; a second system stretches across the central region (Fig. 3). Grooves range up to 4 km in length and from 100 to 350 m in width, with depths of probably no more than a few tens of meters. They range from having beaded outlines, suggesting a series of coalescing pits, to having sharply linear forms. Some grooves intersect craters, but they rarely intersect each other or bifurcate. They show no preferred orientation with respect to local slopes. Although comparable in morphology to grooves on Phobos and Gaspra, the global organization of Ida's grooves is less clearly defined than on these other objects (15). Because at least one groove terminates adjacent to a large block, a subset of grooves may simply be boulder tracks. In addition, grooves may be the surface expressions of massive planar fractures and joints in possible underlying bedrock of Ida, caused by the stress of large impacts.

Albedo stripes and patches are seen within the large craters of the eastern region and are commonly oriented downslope, although it is difficult to separate true albedo variations from abrupt changes in local slopes at projected ridge lines. Generally, stripes are 50 to 100 m wide and range from 400 m to 4 km in length. These features may be the courses of optically immature regolith exposed during downslope movement, although some could be grooves or rays of ejecta from a hidden crater. There is a bright triangular feature 2.5 km long and 500 m wide in the eastern region (Fig. 3), which could be the result of downslope movement of surface materials. There is also at least one dark feature besides the dark-floored craters.

Chutes. Inside the rim of one 8-km crater, we have found three shallow depressions located upslope from small degraded craters. The largest is 1 km long and 400 m wide, and they all appear to be shallow. They probably are scars produced by failure

of weak material on an oversteepened slope triggered by an impact. This again may imply the presence of a regolith.

Regolith. There is abundant evidence for a regolith on Ida. The downslope orientation of chutes and bright stripes, the morphology of pitted grooves, the range of crater morphologies, dark-floored craters, and craters with bright rims are all most simply explained in terms of a ubiquitous regolith. The size of craters showing flat-bottomed topography suggests a regolith depth, in those localities, of a few hundred meters. Photometric studies, which may clarify the relation of all these features to the properties of the regolith, must await a more accurate shape model, which can be derived only after images with complete rotational coverage are analyzed.

Comparisons with Gaspra

Both objects share an elongated, irregular shape, apparently with at least some large planar facets. Grooves exist on both asteroids. The two asteroids show major differences in their cratering records and in the nature of their surface layers. Ida's surface has been exposed to sufficient cratering to have reached equilibrium, at least for craters up to diameters of ~1 km. Unlike Gaspra (3, 4), Ida has many large craters up to a sizable fraction (~0.7) of Ida's mean radius. As a recorder of cratering, Gaspra's surface appears to have been "reset" at least once (that is, all preexisting craters seem to have been destroyed, perhaps by shaking caused by a large impact), and the present population of resolved craters (>100 m in diameter) is so sparse that it represents the production function. On the basis of the reasonable assumptions that the cratering rate and size distribution of impacting objects should be similar at Ida and Gaspra (11) and that both bodies have similar impact strengths, Ida's surface must be much older (perhaps 5 to 10 times) than Gaspra's. Ida's largest impacts failed to have the resetting effects observed on Gaspra, possibly reflecting that the response to such events depends on body size.

Although they share many geologic features (for example, craters, grooves, and regolith), Ida shows a greater range of geological features than Gaspra. This may be because of the presence of deeper regolith on Ida, whose stronger gravity naturally retains a greater fraction of ejecta; an indication of this may be the presence of a few possible rayed craters on Ida but not on Gaspra. A second factor is Ida's longer lifetime against catastrophic disruption, which we estimate at 1.5 billion years, versus 500 million years for Gaspra (16). The asteroid has survived long enough to both generate and accumulate more ejecta on its surface.

It remains to be seen whether the two asteroids have similar photometric and spectral properties when compared at high spatial resolution. Globally integrated ground-based spectrophotometric data indicate that intriguing albedo and spectral variations may be present on the largest scale on Ida (6). This suggests that compositional contrasts may also be present on this object that are even more extreme than those on Gaspra, despite the homogeneity already reported for this face of Ida by the Galileo Near-Infrared Mapping Spectrometer investigators (17). Images that provide data on color and on the true shape of the object have already been returned, between February and June 1994, and are undergoing analysis.

REFERENCES AND NOTES

1. Ida is an S-type (18) main-belt asteroid and a member of the Koronis family (19). Ground-based observations (6) indicate an elongated object (axial ratios $a/b = 1.82$ and $b/c = 1.15$) with mean diameter ~28 km and geometric albedo 0.25. It has retrograde spin with a period of 4.633 hours about an axis that points in one of two possible directions (6), indistinguishable in telescopic data. Variations observed during a rotation period indicate possible albedo (6) and compositional variations (20) across its surface. The brighter members of the Koronis family are taxonomically homogeneous (21), and the observed distribution of spin states has been interpreted in terms of a young age for the Koronis family relative to the age of the solar system (12).
2. Galileo encountered Ida at UT 16:52:05 on 28 August 1993, at a heliocentric distance of 2.95 astronomical units. The spacecraft flew south of the asteroid (~75° S ecliptic latitude) at a speed of 12.4 km/s and a range of 2400 km.
3. M. J. S. Belton *et al.*, *Science* **257**, 1647 (1992); J. Veverka *et al.*, *Icarus* **107**, 2 (1994); M. H. Carr *et al.*, *ibid.*, p. 61; P. C. Thomas *et al.*, *ibid.*, p. 23; C. R. Chapman *et al.*, *ibid.*, in press; M. E. Davies *et al.*, *ibid.* **107**, 18 (1994); P. Helfenstein *et al.*, *ibid.*, p. 37; R. Greenberg *et al.*, *ibid.*, p. 84.
4. J. Veverka *et al.*, *Icarus* **107**, 72 (1994).
5. M. J. S. Belton *et al.*, *Space Sci. Rev.* **60**, 413 (1992).
6. R. P. Binzel *et al.* [*Icarus* **105**, 310 (1993)], M. Gonnano-Beurer *et al.* [*Astron. Astrophys.* **254**, 393 (1992)], and D. J. Tholen (private communication) provided the Galileo project with an estimate of the mean diameter and geometric albedo.
7. Because of its shape and rotation, Ida's effective surface gravity must vary by as much as a factor of 2 across its surface. For a density of 3.5 g/cm³, we estimate a mean surface gravity of ~1.4 cm/s². Centrifugal accelerations of ~0.4 cm/s² apply at the ends of the asteroid.
8. Craters >500 m in diameter were identified, classified, and measured in a region of ~320 km², mostly in the central region where the lighting is good and the slant angle not too great. Craters down to about one-third that size were studied in a 25-km² sub-region (craters <100 m in diameter are visible in the image but have not been examined in this preliminary study). A larger area (723 km²) was used to obtain better statistics for craters 1 to 4 km in diameter. There were about 470 craters in the total sample; the image scale (used for crater diameters and area calculation) was known to about 5% when these studies were done.
9. C. R. Chapman, J. A. Mosher, G. Simmons, *J. Geophys. Res.* **75**, 1445 (1970).
10. W. K. Hartmann, *Icarus* **60**, 56 (1984).
11. W. F. Bottke Jr., M. C. Nolan, R. Greenberg, R. A. Kolvoord, *ibid.* **107**, 255 (1994).
12. R. P. Binzel, *ibid.* **100**, 274 (1992); thesis, University of Texas, Austin (1986); *Icarus* **73**, 303 (1988).

13. S. W. Lee *et al.*, *Icarus* **68**, 77 (1986).
14. Using the rate-dependent strength-scaling law from K. R. Housen and K. A. Holsapple [*ibid.* **84**, 226 (1990)] and an rms collision velocity of 3.92 km/s (11) and assuming that half of the energy is partitioned into disruption of the target, we find that blocks 30 to 100 m in diameter can be disrupted by impactors that are 1.3 to 4 m in diameter. The adopted collision probability (11) is $3.8 \times 10^{-18} \text{ km}^{-2} \text{ year}^{-1}$. Assumption of a power-law exponent of -4.0 for small projectiles yields 30 million to 80 million years for block lifetime against disruption (possibly younger if there are enhanced collisions by Koronis family asteroids). These results are in accord with meteorite exposure ages (22), which suggest that meter-sized objects survive a few tens of millions of years.
15. P. Thomas *et al.*, *J. Geophys. Res.* **84**, 8457 (1979); (4). Because recognizability of lineaments can be strongly influenced by the single azimuth of illumination geometry, our knowledge of lineament orientations may be strongly biased.
16. Using the Holsapple scaling law [K. A. Holsapple, *Annu. Rev. Earth Planet. Sci.* **21**, 333 (1993)] with an experimentally measured gravitational self-compression term (plus other assumptions) as in (14), we estimate that Ida can be shattered by a projectile 1.7 km in diameter. Ida is in the size range at which the collisional energy needed to shatter it is comparable to that needed for fragments to escape from Ida's gravity. Thus, the lifetime against dispersal is about the same as the lifetime against shattering. Here we assume that Ida responds to collisions as if it were a strong rocky body; the uncertainties in the lifetime of 1.5 billion years are at least a factor of 2, mostly because of the uncertainties in (i) the effective strength and (ii) the asteroid size distribution at sizes between 1 and 25 km.
17. R. W. Carlson *et al.*, *Eos* **74** (no. 43), 384 (1993).
18. D. J. Tholen, in *Asteroids II*, R. P. Binzel *et al.*, Eds. (Univ. of Arizona Press, Tucson, 1989), pp. 1139–1150.
19. K. Hirayama, *Astron. J.* **31**, 185 (1918); A. Carusi and G. B. Valsecchi, *Astron. Astrophys.* **115**, 327 (1982); V. Zappala *et al.*, *Astron. J.* **100**, 2030 (1990); J. G. Williams, *Icarus* **96**, 251 (1992).
20. M. A. Barucci and M. Lazzarin, *Bull. Am. Astron. Soc.* **25**, 1139 (1993).

21. J. C. Gradle *et al.*, in *Asteroids*, T. Gehrels, Ed. (Univ. of Arizona Press, Tucson, 1979), pp. 359–390; R. P. Binzel and S. Xu, *Icarus* **106**, 608 (1993).
22. D. Bogard, in *Asteroids*, T. Gehrels, Ed. (Univ. of Arizona Press, Tucson, 1979), pp. 558–578.
23. We thank the Galileo project and the National Aeronautics and Space Administration (NASA) for support; in particular, the Galileo Flight Team, led by W. O'Neil, N. Ausman, M. Landano, and O. Adams. The Ida mosaic was constructed by L. Wainio's group and we wish to recognize H. Mortensen. We also acknowledge D. J. Tholen, R. P. Binzel, P. Magnusson, A. Barucci, S. Mottola, R. Sullivan, R. Pappalardo, P. Geissler, J.-M. Petit, J. Moore, W. F. Bottke, M. Nolan, E. Ryan, W. Merline, B. E. A. Mueller, E. Asphaug, B. Carcich, P. Lee, D. Simonelli, R. Wagner, P. J. Guske, J. Yoshimizu, and R. Hasegawa. A portion of this research was carried out at the Jet Propulsion Laboratory, California Institute of Technology, under contract with NASA. The National Optical Astronomy Observatories are operated by the Association of Universities for Research in Astronomy, Inc. (AURA), under cooperative agreement with the National Science Foundation.

Catastrophes, Phase Shifts, and Large-Scale Degradation of a Caribbean Coral Reef

Terence P. Hughes

Many coral reefs have been degraded over the past two to three decades through a combination of human and natural disturbances. In Jamaica, the effects of overfishing, hurricane damage, and disease have combined to destroy most corals, whose abundance has declined from more than 50 percent in the late 1970s to less than 5 percent today. A dramatic phase shift has occurred, producing a system dominated by fleshy macroalgae (more than 90 percent cover). Immediate implementation of management procedures is necessary to avoid further catastrophic damage.

Coral reefs are renowned for their spectacular diversity and have significant aesthetic and commercial value, particularly in relation to fisheries and tourism. However, many reefs around the world are increasingly threatened, principally from overfishing and from human activities causing excess inputs of sediment and nutrients such as pollution, deforestation, reef mining, and dredging (1). There is a pressing need to monitor coral reefs to assess the spatial and temporal scale of any damage that may be occurring and to conduct research to understand the mechanisms involved.

Here I describe dramatic shifts in reef community structure that have largely destroyed coral reefs around Jamaica. The results presented here summarize the most comprehensive reef monitoring program yet conducted in the Caribbean, in which annual censusing has been carried out for 17 years at multiple sites and depths along 300

km of coastline. In addition, Jamaican reefs are among the best studied in the world, with a wealth of information available on marine ecology and reef status since the 1950s (2). These long-term observations provide a basis for evaluating the role of rare events such as hurricanes and for quantifying gradual trends in coral cover and diversity over a decadal time scale.

Jamaica (18°N, 77°W) is the third largest island in the Caribbean and lies at the center of coral diversity in the Atlantic Ocean (2). Over 60 species of reef-building corals occur there, four of which are spatial dominants: branching elkhorn and staghorn corals, *Acropora palmata* and *Acropora cervicornis*, which form two distinctive zones on the shallow fore-reef; massive or platelike *Montastrea annularis*, the most important framework coral; and encrusting or foliose *Agaricia agaricites* (3). Reefs fringe most of the north Jamaican coast along a narrow (<1 to 2 km) belt and occur sporadically on the south coast on a much broader (>20 km) shelf. Sea-grass beds and mangrove are

often closely associated with reefal areas and provide significant nurseries for commercially important reef fisheries (4). Similar ecosystems, with minor variations in community composition, occur throughout the Caribbean (2).

Jamaica's population growth trajectory is typical of most Third World countries (Fig. 1). The population was less than half a million before 1870, then doubled by 1925 and again by 1975, rising to 2.5 million today. Exponential growth continues, with a further 20% increase expected in the next 15 years (5). Environmental changes on land are conspicuous, with virtually all of the native vegetation having been cleared for agriculture and urban development. Major transformations are also occurring on Jamaica's coral reefs.

Overfishing (1960s to Present)

Chronic overfishing is an ever increasing threat to coral reefs worldwide as coastal populations continue to grow (for example, Fig. 1) and exploit natural resources (6). Extensive studies in Jamaica by Munro (7) showed that by the late 1960s fish biomass had already been reduced in preceding dec-

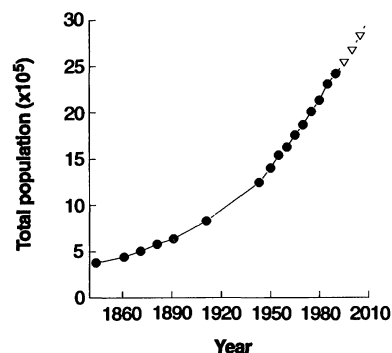


Fig. 1. Population growth of Jamaica, based on numerous sources (5).

The author is in the Department of Marine Biology, James Cook University, Townsville, QLD 4811, Australia.